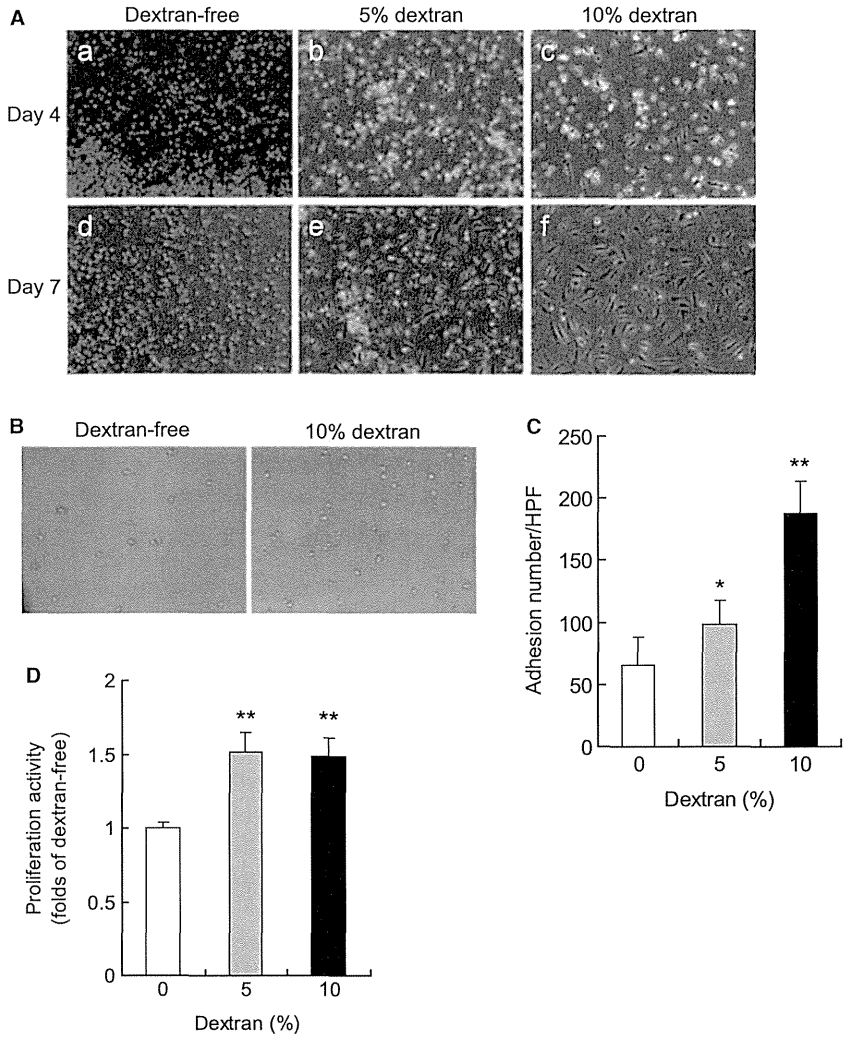

Figure 1. Effect of dextran on the culture, adhesion, and proliferation. $3 \times 10^4/cm^2$ floating endothelial progenitor cells (EPCs) were cultured in medium with 5% dextran (A-b and -e) and 10% dextran (A-c and -f) or without dextran (A-a and -d) on human fibronectin-coated dishes. After 4 days (A-a, -b, and -c) and 7 days (A-d, -e, and -f) EPCs were observed by a phase contrast microscope (×10) (A). Dextran induced differentiation of circulating EPCs toward adhesive EPCs. Floating EPCs exposed to various densities of dextran for 24 h were cultured for 6 h and the adhesive cells were observed by a phase contrast microscope (×10) (B). EPCs exposed to dextran significantly increased adhesion. The number of adhesive cells per high-power field (HPF) was counted (C). $N = 3$. Floating EPCs exposed to various density of dextran for 24 h were cultured for 24 h and the proliferation activity was measured (D). Dextran increased proliferation. $N = 5$. Data are means ± SD. $^{**}P < 0.01$, $^{*}P < 0.05$ versus dextran-free control.

Floating EPCs were exposed to 5% and 10% dextran for 48 h, and changes in the mRNA levels of the endothelial markers VEGF-R1, VEGF-R2, VE-cadherin, and Tie2, and angiogenic factors eNOS, MMP9, and VEGF were analyzed by real-time PCR. The expression levels of these genes markedly increased in response to dextran (Fig. 3B).

These findings suggest that dextran increases the surface expression levels of endothelial marker proteins by affecting those genes and induces floating-circulating EPCs into endothelial differentiation.

Dextran increases gene expression levels of endothelial cell-related transcription factors

Floating EPCs were exposed to 10% dextran for 48 h, and 69 representative mRNA expression levels of the transcription factors expressing in embryonic endothelial cells were analyzed by real-time PCR (Fig. 4A). Thirteen genes in dextran EPCs increased more than 1.5 fold, whereas nine genes in dextran EPCs decreased less than 0.67 fold. Dextran significantly increased the mRNA expression levels of endothelium-related transcription factors ID1/2,

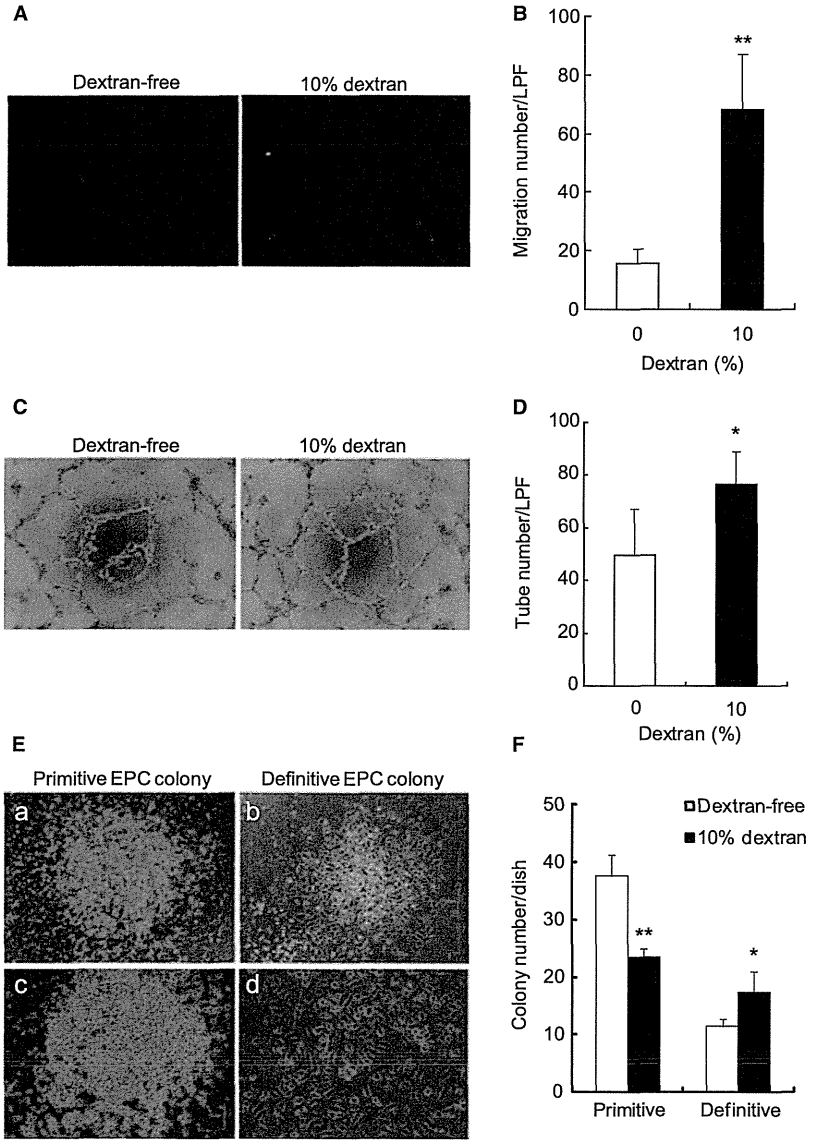

Figure 2. Effect of dextran on the migration, tube formation, and endothelial progenitor cell (EPC) colony formation. Floating EPCs were cultured with or without 10% dextran for 24 h and they were used for measuring following bioactivities. Nuclei of migrated EPCs were stained with DAPI (×10) (A). The number of migrated cells was counted (B). Dextran increased migration. $N = 3$. EPCs under exposure of dextran for 24 h were cultured in matrigel with HUVECs and were observed by a phase contrast microscope (×4) (C). Dextran apparently increased tube formation. The number of tubes per low power field (LPF) was measured (D). $N = 5$. EPCs were cultured in methylcellulose-containing medium for 15 days, and EPC colonies were observed (E-a and -b, x4; E-c and -d, ×10). Representative pictures of a primitive EPC colony (E-a and -c) and a definitive EPC colony (E-b and -d). Dextran decreased the number of primitive EPC colonies and increased that of definitive EPC colonies (F). $N = 3$. Data are means ± SD. $^{**}P < 0.01$, $^{*}P < 0.05$ versus dextran-free control.

FOXM1, HEY1, SMAD1, FOSL1, NFkB1, NRF2, HIF1A, and EPAS1 (Fig. 4B). On the other hand, dextran significantly decreased those of hematopoietic- and anti-angiogenic-related transcription factors TAL1, RUNX1, c-MYB, GATA1/2, ERG, FOXH1, HHEX, and SMAD2/3 (Fig. 4C). These findings indicate that dextran increases both protein and mRNA expression levels of endothelial markers by affecting transcription factors.

Multiple signal transduction pathways regulate proliferation, adhesion, tube formation, and differentiation

To investigate which signal transduction pathways take part in proliferation, adhesion, tube formation, and differentiation in response to dextran, inhibitors of signal transduction pathways were added in those assays.

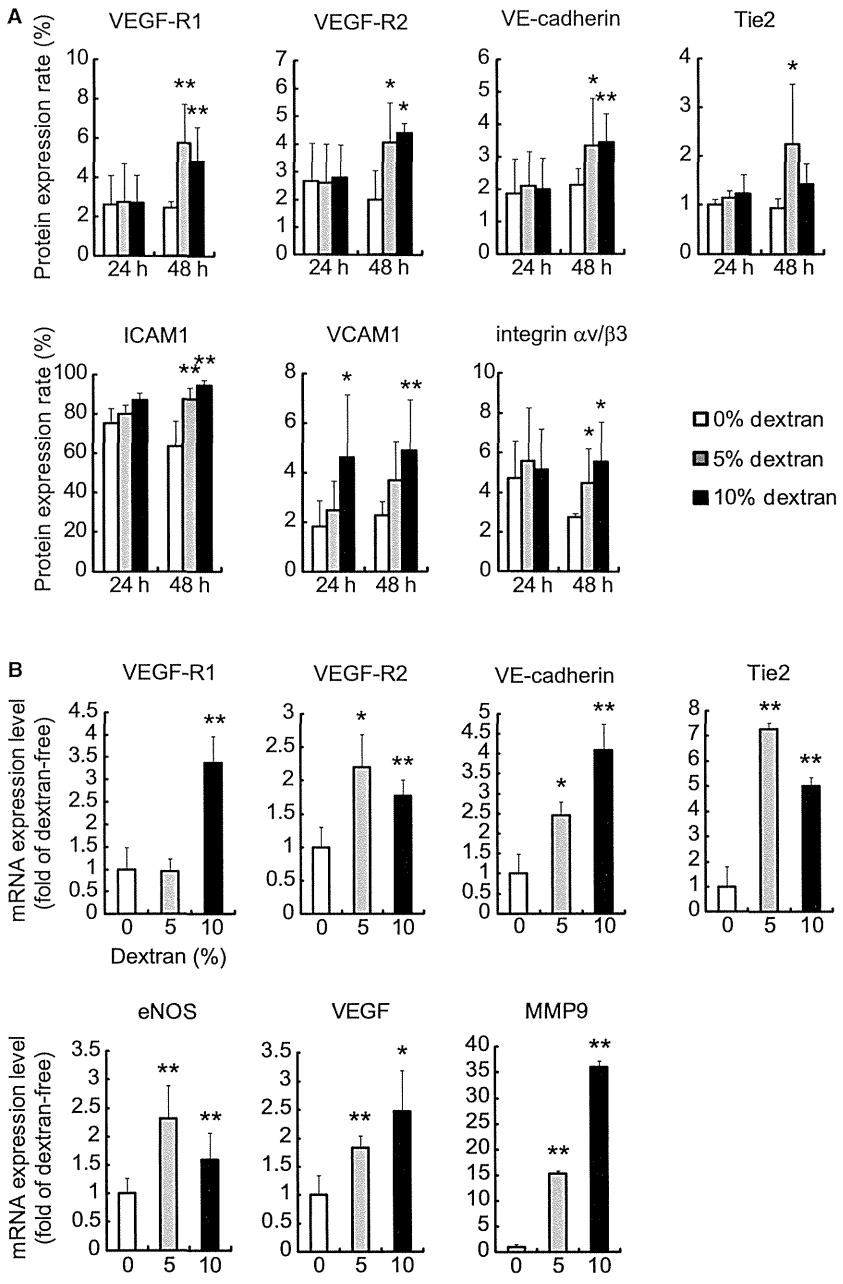

Figure 3. Effect of dextran on the protein and mRNA expression levels of endothelial markers. The expression rates of surface protein in floating endothelial progenitor cells (EPCs) under exposure of 5% and 10% dextran for 24 h (24 h) or 48 h (48 h) were analyzed (A). In 24 h-EPCs, 10% dextran increased the protein expression of VCAM1. In 48 h-EPCs, 5% and/or 10% dextran increased vascular endothelial growth factor (VEGF)-R1, VEGF-R2, VE-cadherin, Tie2, ICAM1, VCAM1, and integrin αv/β3. The mRNA expression levels of EPCs under exposure of 5% and 10% dextran for 48 h were analyzed (B). 5% and/or 10% dextran increased gene expression levels of VEGF-R1, VEGF-R2, VE-cadherin, Tie2, endothelial nitric oxide synthase, MMP9, and VEGF. Values are means ± SD of five samples. $^{**}P < 0.01$, $^{*}P < 0.05$ versus dextran-free control.

LY294002, PD98059, JNK inhibitor II, and SB203580 were used as the specific inhibitors of phosphoinositide 3-kinase (PI3K), extracellular signal-regulated kinase 1/2 (ERK1/2), c-Jun N-terminal kinase (JNK), and p38 mitogen-activated protein kinase (p38), respectively.

A proliferation assay and an adhesion assay with inhibitors showed that every inhibitor decreased the proliferation activity and the adhesive cell number (Fig. 5A and B). These results indicate that PI3K/Akt, ERK1/2, JNK, p38 pathways increase bioactivi-

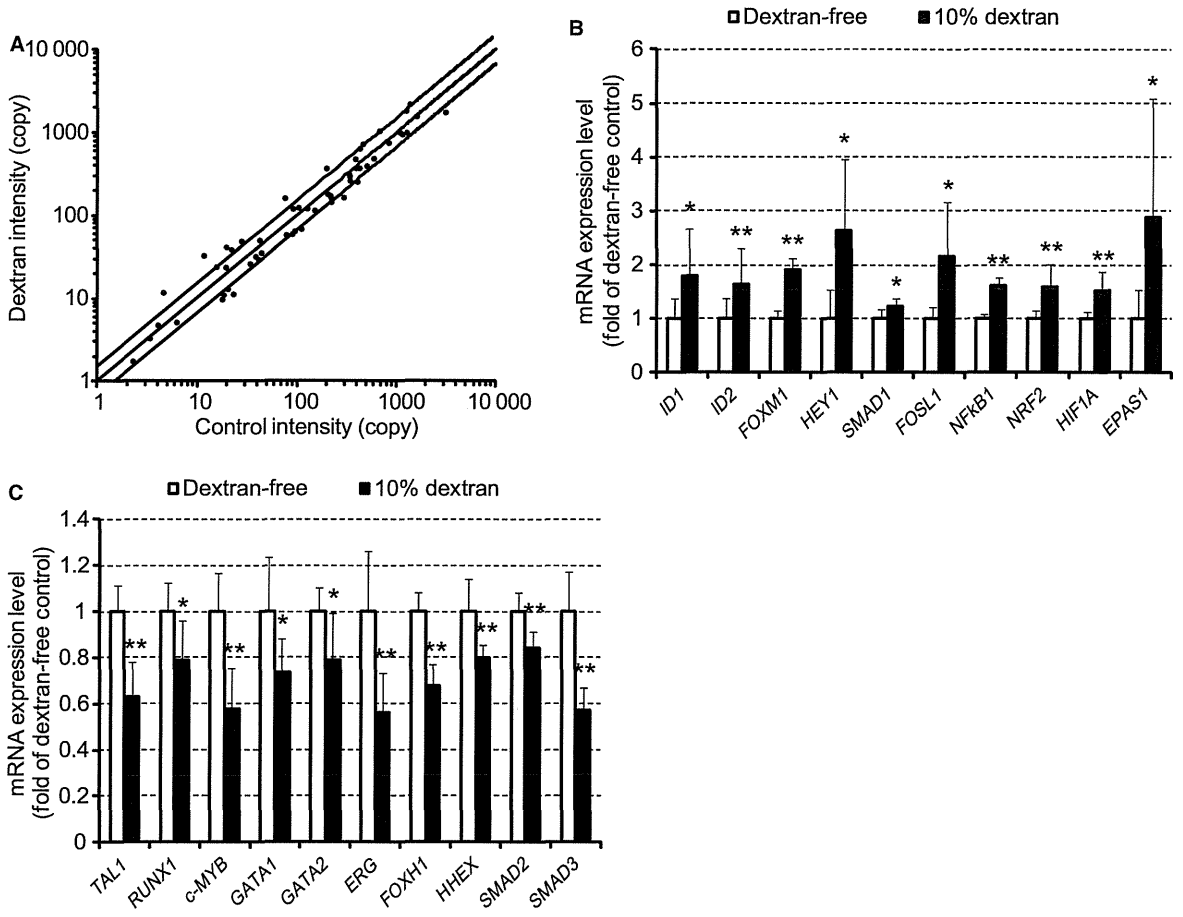

Figure 4. Effect of dextran on the transcription factors. The mRNA expression levels of transcription factors in floating EPCs under exposure of 10% dextran for 48 h were analyzed. Expression levels of 69 genes per 10,000 GAPDH copies are shown in A. The horizontal (*x*) axis indicates copy number in dextran-free EPCs (control intensity). The vertical (*y*) axis indicates copy number in dextran EPC (dextran intensity). The lines display $y = 1.5x$, $y = x$, and $y = 2/3\,x$, respectively. Relative expression levels of 10 selected genes are shown in B and C. Dextran increased gene expression levels of ID1/2, FOXM1, HEY1, SMAD1, FOSL1, NFkB1, NRF2, HIF1A, and EPAS1. While dextran decreased those of TAL1, RUNX1, c-MYB, GATA1/2, ERG, FOXH1, HHEX, and SMAD2/3. $N = 5$. Data are means ± SD. $^{**}P < 0.01$, $^{*}P < 0.05$ versus dextran-free control.

ties of proliferation and adhesion in response to dextran.

A tube formation assay showed that the ERK1/2, JNK, p38 inhibitors suppressed tube formation, whereas the PI3K inhibitor did not change it significantly (Fig. 5C). This suggests that ERK1/2, JNK, and p38 pathways increase the dextran-responsive tube formation.

A colony assay indicated that every inhibitor increased the number of primitive EPC colonies; on the other hand, it decreased the number of definitive EPC colonies (Fig. 5D). This means that PI3K/Akt, ERK1/2, JNK, and p38 are involved in the dextran-inducing differentiation.

To confirm how signal transduction pathways regulate differentiation of EPCs, EPCs with inhibitors were exposed to 10% dextran for 48 h and endothelial marker genes were analyzed. A real-time PCR analysis showed that the PI3K inhibitor decreased mRNA expression levels of VEGF-R1 and eNOS (Fig. 5E). The ERK1/2 inhibitor decreased those of VEGF-R1, VE-cadherin, Tie2, and eNOS. The JNK inhibitor decreased those of VEGF-R1, VE-cadherin, and eNOS. The p38 inhibitor decreased those of VEGF-R2, VE-cadherin, and eNOS, on the other hand, increased that of Tie2. These results indicate that PI3K/Akt, ERK1/2, JNK, and p38 pathways complicatedly regulate the EPC differentiation in response to dextran.

Discussion

We have developed an epoch-making EPC differentiation assay. The results of this study showed that dextran enlarged the bioactivities of adhesion, migration, proliferation, and tube formation, as the mRNA expression levels

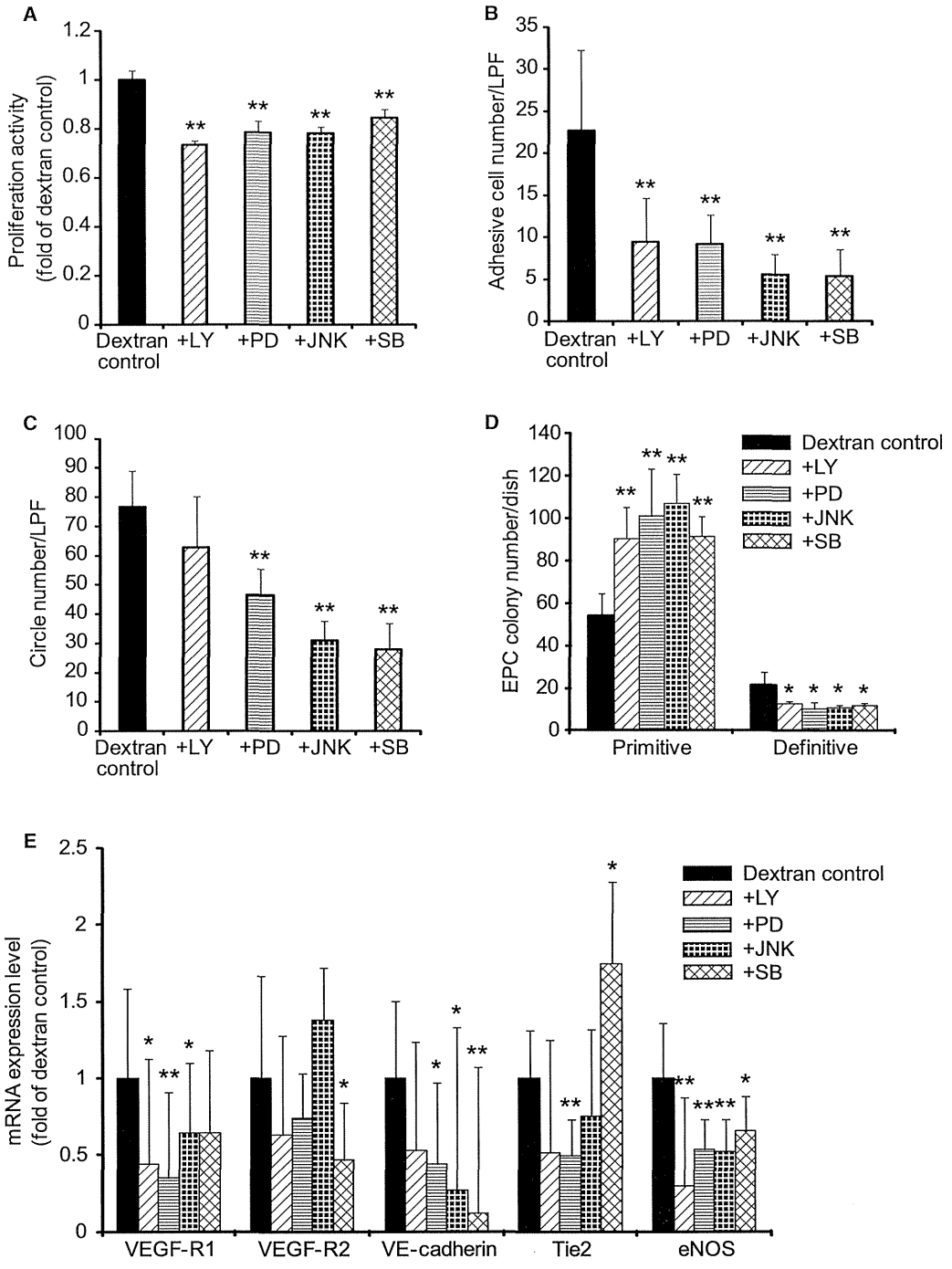

Figure 5. Inhibitor analysis of the adhesion, proliferation, tube formation, endothelial progenitor cell (EPC) colony formation, and differentiation. The abilities of proliferation (A), adhesion (B), tube formation (C), and EPC colony formation were analyzed (D) after floating EPCs were exposed to 10% dextran for 24 h with various inhibitors of signal transduction pathways,. All inhibitors decreased proliferation and adhesion. PD98059, JNK inhibitor II, and SB203580 decreased tube formation. Every inhibitor decreased definitive EPC colony formation, meanwhile, increased primitive EPC colony formation. EPCs were exposed to 10% dextran for 48 h with various inhibitors and the mRNA expression levels were analyzed (E). Inhibitors decreased almost all mRNA expression levels of vascular endothelial growth factor (VEGF)-R1, VEGF-R2, VE-cadherin, Tie2, and endothelial nitric oxide synthase. However, SB203580 increased the mRNA expression level of Tie2. LY, LY294002; PD, PD98059; JNK, JNK inhibitor II; and SB, SB203580. Values are means ± SD of 3–5 samples. $^{**}P < 0.01$, $^{*}P < 0.05$ versus dextran control.

of angiogenic factors, eNOS, MMP9, and VEGF genes increased in floating EPCs cultured in a suspended manner. In addition, dextran increased both protein and gene expression levels of the endothelial markers VEGF-R1, VEGF-R2, VE-cadherin, and Tie2, and activated endothelial markers ICAM1, VCAM1, and integrin αv/β3. Dextran increased differentiating definitive type of EPC colony-forming cells instead of primitive EPC colony-forming cells. These findings indicate that dextran induces circulating EPCs toward mature adhesive EPCs.

Dextran has various influences on cell bioactivities through changing osmolality and viscosity, and binding with macrophage mannose receptor (MMR). In addition, dextran may be capable of presenting scaffold and differentiation-related molecules to cells. There are integrins, the cytoskeleton, receptor tyrosine kinases, and transient receptor potential (TRP) channels which sense osmolality and transmit the information into inner cells (Pedersen et al. 2011). Cell swelling increases integrin β1 followed by Rho activity. The actin cytoskeleton reorganizes rapidly using Rho family G proteins, nonmuscle myosin II, cortactin, and the WASP/Arp2/3 system in response to osmotic stress. Hypotonic swelling activates epidermal growth factor receptor with integrin. TRPV4 displays hypotonicity-induced calcium influx. However, the change in the medium osmolality in this study by 10% dextran is less than 5% and the values of osmolality are within physiological state. Viscosity is generated by macrorheological parameters, hematocrit and serum proteins like fibrinogen and globulins, and microrheological parameters, the degree of red blood cells aggregation and deformability under blood- and tissue-flow condition. Impairment of responses to viscosity leads to the development of various vascular diseases such as hypertension (Koenig et al. 1989), diabetes (Skovborg et al. 1966; Cho et al. 2008), strokes, and ischemic heart diseases (Lowe et al. 1997). The blood viscosity is about 3.5 cP (Ercan et al. 2002; Lo Presti et al. 2002; Marcinkowska-Gapińska and Kowal 2006) and the viscosity in bone marrow is 37.5 cP (Gurkan and Akkus 2008). In this study, the viscosity of control medium, medium with 5% dextran, and medium with 10% dextran is about 1, 3.5, and 8 cP, respectively. The viscosity change by 5% or 10% dextran is not likely significant for the physiological environment in which EPCs exist. MMR is expressed in the endothelial cells in embryo and adult, macrophages, and dendritic cells (Sallusto et al. 1995; Takahashi et al. 1998; Gröger et al. 2000). MMR is a 175 kDa transmembrane glycoprotein characterized by a cysteine-rich NH_2-terminal domain, eight C-type lectin carbohydrate recognition domains with broad specificity for sugars, and a cytoplasmic tail related to endocytosis and phagocytosis (Ezekowitz et al. 1990; Stahl 1992; Taylor and Drickamer 1993). MMR-knockout mice show that high amounts of mannose and N-acetylglucosamine reside in serum and that elevated levels of lysosomal hydrolases exist in serum, suggesting that MMR regulates serum glycoprotein homeostasis (Lee et al. 2002). MMR is expressed in M2 macrophages which secrete cytokines including interleukin 10, chemokine, cc motif, ligand 17 (CCL17), CCL22, transforming growth factor beta (TGFβ) and promote tissue repair and angiogenesis (Fairweather and Cihakova 2009). This study shows that dextran increases protein expression levels of integrin αv/β3 in floating-circulating EPCs. This suggests that EPCs may recognize dextran as scaffold. Furthermore, dextran may serve more differentiation-related molecules into EPCs. Considering the above-mentioned, elucidation of the stimulation mechanism by dextran would provide deeper insight into the mechanism of bioactivities and differentiation of EPCs.

There are some EPC studies reporting that transcription factors such as SP1, ID1, HIF1A, FOXO3A, KLF4 affected differentiation of EPCs. We have previously demonstrated that shear stress increased the expression level of arterial marker ephrinB2 by activating SP1 in adhesive EPCs (Obi et al. 2009). Conditional ID1 suppression in EPCs impaired the mobilization of EPCs and angiogenesis (Mellick et al. 2010). Knockdown of HIF1A decreased the expression of VEGF, CD31, VEGF-R2, and eNOS and the production of NO in adhesive EPCs (Jiang et al. 2006). Expression of FOXO3A was down regulated in differentiated adhesive EPCs, while overexpression of FOXO3A reduced the number of differentiated adhesive EPCs (Mogi et al. 2008). Overexpression of KLF4 in adhesive EPCs increased CD34 expression and decreased tube formation (Li et al. 2012a).

This study showed that dextran increased mRNA expression levels of ID1/2, FOXM1, HEY1, SMAD1, FOSL1, NFkB1, NRF2, HIF1A, and EPAS1 in circulating EPCs. However, dextran decreased those of hematopoietic- and anti-angiogenic-related transcription factors, such as TAL1, RUNX1, c-MYB, GATA1/2, ERG, FOXH1, HHEX, and SMAD2/3.

ID1 increases proliferation, migration, and tube formation through transcriptional activation of VEGF by stabilizing HIF1A protein (Lee et al. 2006). ID1 also increases adhesion and tube formation through integrin β and Rho kinase signaling (Qiu et al. 2011). ID1 and ID3 double knockout mice show vascular malformations indicating that ID regulates vascular differentiation (Lyden et al. 1999). FOXM1 increases proliferation, migration, and angiogenesis by inducing VEGF and MMP9 (Ahmad et al. 2010). FOXM1 knockout mice display defects in the formation of peripheral pulmonary capillaries (Kim et al. 2005). HEYs function as downstream targets of arterial endothelium marker Notch signaling pathway and HEY1

is induced by bone morphogenetic protein (BMP) and Notch signaling pathway (Itoh et al. 2004). SMADs function as downstream targets of TGFβ and BMP signaling pathways. SMAD1 and SMAD5 lead to ID1 expression and induce proliferation, migration, and tube formation. While, SMAD2 and SMAD3 lead to plasminogen activator inhibitor 1 expression and inhibit proliferation, migration, and tube formation (Scharpfenecker et al. 2009). FOSL1 knockout mice lack a properly vascularized labyrinth layer of placentas (Schreiber et al. 2000). NFkB is a master regulator of inflammation-related gene expression such as ICAM1 and VCAM1. It is reported that ID1/PI3K/Akt/NFkB/survivin signaling pathway increases proliferation of EPCs (Li et al. 2012b). NRF2 regulates gene expressions of antioxidant and anti-inflammation (Mann et al. 2007). HIF1A and EPAS1 are the key factors of angiogenesis in a low oxygen environment although there are many reports in which HIF1A is regulated through oxygen-independent factors including interleukin 1 beta, TGFβ1, insulin-like growth factor 2 (Zelzer et al. 1998; Görlach et al. 2001; Jung et al. 2003). TAL1, RUNX1, c-MYB, GATA1/2, and ERG are representative markers of the HSC lineage (Doré and Crispino 2011). FOXH1 and HHEX inhibit the transcription of VEGF-R2 and suppress angiogenesis (Minami et al. 2004; Choi et al. 2007).

Taken together, these transcription factors are important for EPC differentiation. Further studies of interaction among these transcription factors will elucidate the differentiation process and the origin of EPCs as well as developmental endothelial cells.

Previous studies have reported that the PI3K/Akt signaling pathway regulates the differentiation of circulating EPCs; mechanical shear stress induces endothelial differentiation of circulating EPCs via the PI3K/Akt/mTOR pathway (Obi et al. 2012), and ginsenoside Rg3 decreases differentiation of circulating EPCs via the Akt/eNOS pathway (Kim et al. 2012). This study showed that dextran induced differentiation of circulating EPCs toward adhesive EPCs through multiple signal transductions including PI3K/Akt, ERK1/2, JNK, and p38 (Fig. 6). It is reported that dextran binds with MMR in dendritic cells and is taken up by endocytosis via the mTOR, JNK, and p38 signaling pathways (Arrighi et al. 2001; Hackstein et al. 2002; Nakahara et al. 2004). Clarification of the differences in these pathways would lead to a better understanding of the molecular mechanism by which dextran regulates differentiation of circulating EPCs.

Many studies have demonstrated that circulating EPCs are influenced by physiological and pathological factors such as age, estrogen, exercise, smoking, hypertension, hyperlipidemia, diabetes mellitus, myocardial ischemia, heart failure, and renal failure (Leone et al. 2009). Circulating EPCs are also influenced by drugs including angiotensin-converting enzyme inhibitor, hydroxymethylglutaryl-CoA reductase inhibitor, peroxisome proliferator-activated receptor γ, insulin, erythropoietin, granulocyte colony-stimulating factor (G-CSF). These factors affect mobilization, homing, adhesion, migration, proliferation, and vasculogenesis. Clinically G-CSF is used by EPC transplantation therapy for myocardial ischemia and hind limb ischemia (Li et al. 2007; Losordo et al. 2007; Kawamoto et al. 2009; Lara-Hernandez et al. 2010). This study showed that dextran increased bioactivities of proliferation, adhesion, migration, and tube formation. It suggests that dextran may be effective for the EPC-mediated therapy.

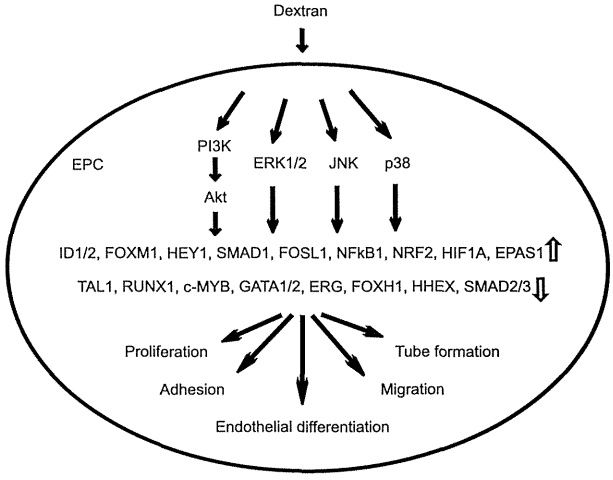

Figure 6. A schematic diagram which shows that dextran induces differentiation of circulating endothelial progenitor cells.

In conclusion, we have made an EPC differentiation assay by using dextran. Dextran increases differentiation, adhesion, migration, proliferation, and vasculogenesis of circulating EPCs. The differentiation mechanism in response to dextran is regulated by multiple signal transductions including PI3K/Akt, ERK1/2, JNK, and p38. The new differentiation assay using dextran will clarify the molecular and physiological mechanisms at successive stages of EPC differentiation from circulation to tissue.

Acknowledgments

We thank Y. Okada and H. Kamiguchi, The Education and Research Support Center, Tokai University for their invaluable support in experimental procedures.

Conflict of Interest

None declared.

References

Aberg, M., and A. Rausing. 1978. The effect of dextran 70 on the structure of *ex vivo* thrombi. Thromb. Res. 12:1113–1122.

Ahmad, A., Z. Wang, D. Kong, S. Ali, Y. Li, S. Banerjee, et al. 2010. FoxM1 down-regulation leads to inhibition of proliferation, migration and invasion of breast cancer cells through the modulation of extra-cellular matrix degrading factors. Breast Cancer Res. Treat. 122:337–346.

Arrighi, J. F., M. Rebsamen, F. Rousset, V. Kindler, and C. Hauser. 2001. A critical role for p38 mitogen-activated protein kinase in the maturation of human blood-derived dendritic cells induced by lipopolysaccharide, TNF-alpha, and contact sensitizers. J. Immunol. 166:3837–3845.

Asahara, T., T. Murohara, A. Sullivan, M. Silver, R. Zee, T. Li, et al. 1997. Isolation of putative progenitor endothelial cells for angiogenesis. Science 275:964–967.

Asahara, T., A. Kawamoto, and H. Masuda. 2011. Circulating endothelial progenitor cells for vascular medicine. Stem Cells 29:1650–1655.

Batlle, J., F. del Río, M. F. López Fernández, R. Martín, and López Borrasca A. 1985. Effect of dextran on factor VIII/von Willebrand factor structure and function. Thromb. Haemost. 54:697–699.

Carlin, G., and T. Saldeen. 1980. On the interaction between dextran and the primary fibrinolysis inhibitor alpha 2-antiplasmin. Thromb. Res. 19:103–110.

Cho, Y. I., M. P. Mooney, and D. J. Cho. 2008. Hemorheological disorders in diabetes mellitus. J. Diabetes Sci. Technol. 2:1130–1138.

Choi, J., L. Dong, J. Ahn, D. Dao, M. Hammerschmidt, and J. N. Chen. 2007. FoxH1 negatively modulates *flk1* gene expression and vascular formation in zebrafish. Dev. Biol. 304:735–744.

Doré, L. C., and J. D. Crispino. 2011. Transcription factor networks in erythroid cell and megakaryocyte development. Blood 118:231–239.

Ercan, M., D. Konukoğlu, T. Erdem, and S. Onen. 2002. The effects of cholesterol levels on hemorheological parameters in diabetic patients. Clin. Hemorheol. Microcirc. 26:257–263.

Ezekowitz, R. A., K. Sastry, P. Bailly, and A. Warner. 1990. Molecular characterization of the human macrophage mannose receptor: demonstration of multiple carbohydrate recognition-like domains and phagocytosis of yeasts in Cos-1 cells. J. Exp. Med. 172:1785–1794.

Fadini, G. P., I. Baesso, M. Albiero, S. Sartore, C. Agostini, and A. Avogaro. 2008. Technical notes on endothelial progenitor cells. Atherosclerosis 197:496–503.

Fairweather, D., and D. Cihakova. 2009. Alternatively activated macrophages in infection and autoimmunity. J. Autoimmun. 33:222–230.

Görlach, A., I. Diebold, V. B. Schini-Kerth, U. Berchner-Pfannschmidt, U. Roth, R. P. Brandes, et al. 2001. Thrombin activates the hypoxia-inducible factor-1 signaling pathway in vascular smooth muscle cells: role of the p22(phox)-containing NADPH oxidase. Circ. Res. 89:47–54.

Gröger, M., W. Holnthoner, D. Maurer, S. Lechleitner, K. Wolff, B. B. Mayr, et al. 2000. Dermal microvascular endothelial cells express the 180-kDa macrophage mannose receptor *in situ* and *in vitro*. J. Immunol. 165:5428–5434.

Gurkan, U. A., and O. Akkus. 2008. The mechanical environment of bone marrow: a review. Ann. Biomed. Eng. 36:1978–1991.

Hackstein, H., T. Taner, A. J. Logar, and A. W. Thomson. 2002. Rapamycin inhibits macropinocytosis and mannose receptor-mediated endocytosis by bone marrow-derived dendritic cells. Blood 100:1084–1087.

Itoh, F., S. Itoh, M. J. Goumans, G. Valdimarsdottir, T. Iso, G. P. Dotto, et al. 2004. Synergy and antagonism between Notch and BMP receptor signaling pathways in endothelial cells. EMBO J. 23:541–551.

Jiang, M., B. Wang, C. Wang, B. He, H. Fan, T. B. Guo, et al. 2006. Inhibition of hypoxia-inducible factor-1alpha and endothelial progenitor cell differentiation by adenoviral transfer of small interfering RNA *in vitro*. J. Vasc. Res. 43:511–521.

Jujo, K., M. Ii, and D. W. Losordo. 2008. Endothelial progenitor cells in neovascularization of infarcted myocardium. J. Mol. Cell. Cardiol. 45:530–544.

Jung, Y. J., J. S. Isaacs, S. Lee, J. Trepel, and L. Neckers. 2003. IL-1beta-mediated up-regulation of HIF-1alpha via an NFkappaB/COX-2 pathway identifies HIF-1 as a critical link between inflammation and oncogenesis. FASEB J. 17: 2115–2117.

Kawamoto, A., M. Katayama, N. Handa, M. Kinoshita, H. Takano, M. Horii, et al. 2009. Intramuscular transplantation of G-CSF-mobilized CD34 (+) cells in patients with critical limb ischemia: a phase I/IIa, multicenter, single-blinded, dose-escalation clinical trial. Stem Cells 27:2857–2864.

Kim, I. M., S. Ramakrishna, G. A. Gusarova, H. M. Yoder, R. H. Costa, and V. V. Kalinichenko. 2005. The forkhead box m1 transcription factor is essential for embryonic development of pulmonary vasculature. J. Biol. Chem. 280:22278–22286.

Kim, J. W., S. Y. Jung, Y. H. Kwon, S. H. Lee, J. H. Lee, B. Y. Lee, et al. 2012. Ginsenoside Rg3 inhibits endothelial progenitor cell differentiation through attenuation of VEGF-dependent Akt/eNOS signaling. Phytother. Res. 26:1286–1293.

Kirton, J. P., and Q. Xu. 2010. Endothelial precursors in vascular repair. Microvasc. Res. 79:193–199.

Koenig, W., M. Sund, E. Ernst, A. Matrai, U. Keil, and J. Rosenthal. 1989. Is increased plasma viscosity a risk factor for high blood pressure? Angiology 40:153–163.

Lara-Hernandez, R., P. Lozano-Vilardell, P. Blanes, N. Torreguitart- Mirada, A. Galmes, and J. Besalduch. 2010. Safety and efficacy of therapeutic angiogenesis as a novel treatment in patients with critical limb ischemia. Ann. Vasc. Surg. 24:287–294.

Lee, S. J., S. Evers, D. Roeder, A. F. Parlow, J. Risteli, L. Risteli, et al. 2002. Mannose receptor-mediated regulation of serum glycoprotein homeostasis. Science 295:1898–1901.

Lee, T. K., R. T. Poon, A. P. Yuen, M. T. Ling, X. H. Wang, Y. C. Wong, et al. 2006. Regulation of angiogenesis by Id-1 through hypoxia-inducible factor-1alpha-mediated vascular endothelial growth factor up-regulation in hepatocellular carcinoma. Clin. Cancer Res. 12:6910–6919.

Leone, A. M., M. Valgimigli, M. B. Giannico, V. Zaccone, M. Perfetti, D. D'Amario, et al. 2009. From bone marrow to the arterial wall: the ongoing tale of endothelial progenitor cells. Eur. Heart J. 30:890–899.

Li, Z. Q., M. Zhang, Y. Z. Jing, W. W. Zhang, Y. Liu, L. J. Cui, et al. 2007. The clinical study of autologous peripheral blood stem cell transplantation by intracoronary infusion in patients with acute myocardial infarction (AMI). Int. J. Cardiol. 115:52–56.

Li, X., Y. Song, D. Wang, C. Fu, Z. Zhu, Y. Han, et al. 2012a. LIF maintains progenitor phenotype of endothelial progenitor cells via Krüppel-like factor 4. Microvasc. Res. 84:270–277.

Li, W., H. Wang, C. Y. Kuang, J. K. Zhu, Y. Yu, Z. X. Qin, et al. 2012b. An essential role for the Id1/PI3K/Akt/NFkB/survivin signalling pathway in promoting the proliferation of endothelial progenitor cells *in vitro*. Mol. Cell. Biochem. 363:135–145.

Lo Presti, R., D. Sinagra, M. Montana, A. M. Scarpitta, A. Catania, and G. Caimi. 2002. Haemorheological profile in metabolic Syndrome. Clin. Hemorheol. Microcirc. 26:241–247.

Losordo, D. W., R. A. Schatz, C. J. White, J. E. Udelson, V. Veereshwarayya, M. Durgin, et al. 2007. Intramyocardial transplantation of autologous CD34 + stem cells for intractable angina: a phase I/IIa double-blind, randomized controlled trial. Circulation 115:3165–3172.

Lowe, G. D., A. J. Lee, A. Rumley, J. F. Price, and F. G. Fowkes. 1997. Blood viscosity and risk of cardiovascular events: the Edinburgh Artery Study. Br. J. Haematol. 96:168–173.

Lyden, D., A. Z. Young, D. Zagzag, W. Yan, W. Gerald, R. O'Reilly, et al. 1999. Id1 and Id3 are required for neurogenesis, angiogenesis and vascularization of tumour xenografts. Nature 401:670–677.

Mann, G. E., D. J. Rowlands, F. Y. Li, P. de Winter, and R. C. Siow. 2007. Activation of endothelial nitric oxide synthase by dietary isoflavones: role of NO in Nrf2-mediated antioxidant gene expression. Cardiovasc. Res. 75:261–274.

Marcinkowska-Gapińska, A., and P. Kowal. 2006. Blood fluidity and thermography in patients with diabetes mellitus and coronary artery disease in comparison to healthy subjects. Clin. Hemorheol. Microcirc. 35:473–479.

Masuda, H., C. Alev, H. Akimaru, R. Ito, T. Shizuno, M. Kobori, et al. 2011. Methodological development of a clonogenic assay to determine endothelial progenitor cell potential. Circ. Res. 109:20–37.

Mellick, A. S., P. N. Plummer, D. J. Nolan, D. Gao, K. Bambino, M. Hahn, et al. 2010. Using the transcription factor inhibitor of DNA binding 1 to selectively target endothelial progenitor cells offers novel strategies to inhibit tumor angiogenesis and growth. Cancer Res. 70:7273–7282.

Minami, T., T. Murakami, K. Horiuchi, M. Miura, T. Noguchi, J. Miyazaki, et al. 2004. Interaction between hex and GATA transcription factors in vascular endothelial cells inhibits flk-1/KDR-mediated vascular endothelial growth factor signaling. J. Biol. Chem. 279:20626–20635.

Mogi, M., K. Walsh, M. Iwai, and M. Horiuchi. 2008. Akt-FOXO3a signaling affects human endothelial progenitor cell differentiation. Hypertens. Res. 31:153–159.

Nakahara, T., H. Uchi, K. Urabe, Q. Chen, M. Furue, and Y. Moroi. 2004. Role of c-Jun N-terminal kinase on lipopolysaccharide induced maturation of human monocyte-derived dendritic cells. Int. Immunol. 16:1701–1709.

Obi, S., K. Yamamoto, N. Shimizu, S. Kumagaya, T. Masumura, T. Sokabe, et al. 2009. Fluid shear stress induces arterial differentiation of endothelial progenitor cells. J. Appl. Physiol. 106:203–211.

Obi, S., H. Masuda, T. Shizuno, A. Sato, K. Yamamoto, J. Ando, et al. 2012. Fluid shear stress induces differentiation of circulating phenotype endothelial progenitor cells. Am. J. Physiol. Cell Physiol. 303:C595–C606.

Pearson, J. D. 2010. Endothelial progenitor cells – an evolving story. Microvasc. Res. 79:162–168.

Pedersen, S. F., A. Kapus, and E. K. Hoffmann. 2011. Osmosensory mechanisms in cellular and systemic volume regulation. J. Am. Soc. Nephrol. 22:1587–1597.

Qiu, J., G. Wang, Q. Peng, J. Hu, X. Luo, Y. Zheng, et al. 2011. Id1 induces tubulogenesis by regulating endothelial cell adhesion and cytoskeletal organization through β1-integrin and Rho-kinase signalling. Int. J. Mol. Med. 28:543–548.

Robless, P. A., T. J. Tegos, D. Okonko, A. O. Mansfield, A. N. Nicolaides, D. P. Mikhailidis, et al. 2002. Platelet activation during carotid endarterectomy and the antiplatelet effect of Dextran 40. Platelets 13:231–239.

Rouleau, L., J. Rossi, and R. L. Leask. 2010. Concentration and time effects of dextran exposure on endothelial cell viability, attachment, and inflammatory marker expression *in vitro*. Ann. Biomed. Eng. 38:1451–1462.

Sallusto, F., M. Cella, C. Danieli, and A. Lanzavecchia. 1995. Dendritic cells use macropinocytosis and the mannose receptor to concentrate macromolecules in the major histocompatibility complex class II compartment: downregulation by cytokines and bacterial products. J. Exp. Med. 182:389–400.

Scharpfenecker, M., J. J. Kruse, D. Sprong, N. S. Russell, P. Ten Dijke, and F. A. Stewart. 2009. Ionizing radiation shifts the PAI-1/ID-1 balance and activates notch signaling in endothelial cells. Int. J. Radiat. Oncol. Biol. Phys. 73:506–513.

Schreiber, M., Z. Q. Wang, W. Jochum, I. Fetka, C. Elliott, and E. F. Wagner. 2000. Placental vascularisation requires the AP-1 component fra1. Development 127:4937–4948.

Skovborg, F., A. V. Nielsen, J. Schlichtkrull, and J. Ditzel. 1966. Blood-viscosity in diabetic patients. Lancet 1:129–131.

Stahl, P. D. 1992. The mannose receptor and other macrophage lectins. Curr. Opin. Immunol. 4:49–52.

Takahashi, K., M. J. Donovan, R. A. Rogers, and R. A. Ezekowitz. 1998. Distribution of murine mannose receptor expression from early embryogenesis through to adulthood. Cell Tissue Res. 292:311–323.

Taylor, M. E., and K. Drickamer. 1993. Structural requirements for high affinity binding of complex ligands by the macrophage mannose receptor. J. Biol. Chem. 268:399–404.

Wieslander, J. B., P. Dougan, U. Stjernquist, M. Aberg, and S. E. Bergentz. 1986a. The influence of dextran and saline solution upon platelet behavior after microarterial anastomosis. Surg. Gynecol. Obstet. 163:256–262.

Wieslander, J. B., P. Dougan, U. Stjernquist, and C. V. Mecklenburg. 1986b. Effect of dextran 70 and saline on thrombus formation following arteriotomy and intimectomy in small arteries. Microsurgery 7:168–177.

Yoder, M. C. 2009. Defining human endothelial progenitor cells. J. Thromb. Haemost. 7(Suppl 1):49–52.

Zelzer, E., Y. Levy, C. Kahana, B. Z. Shilo, M. Rubinstein, and B. Cohen. 1998. Insulin induces transcription of target genes through the hypoxia-inducible factor HIF-1alpha/ARNT. EMBO J. 17:5085–5094.

DOI: 10.3727/096368914X685799

CT-1353 Accepted 12/20/2014 for publication in "Cell Transplantation"

Functional and Electrical Integration of Induced Pluripotent Stem Cell-Derived Cardiomyocytes in a Myocardial Infarction Rat Heart

Short title: Integration of iPSC-cardiomyocytes in the heart

Takahiro Higuchi[1], MD, Shigeru Miyagawa MD, PhD[1], James T. Pearson, PhD[2,3], Satsuki Fukushima MD, PhD[1], Atsuhiro Saito PhD[4], Hirotsugu Tsuchimochi, PhD[5], Takashi Sonobe, PhD[4], Yutaka Fujii, MS[5], Naoto Yagi, PhD[6], Alberto Astolfo, PhD[2], Mikiyasu Shirai, MD PhD[5], Yoshiki Sawa MD, PhD[1]

[1]Department of Cardiac Surgery, Osaka University Graduate School of Medicine, Osaka, Japan, [2]The Australian Synchrotron, Clayton, Victoria Australia, [3]Monash Biomedical Imaging Facility, Monash University, Clayton, Victoria, Australia, [4]Medical Center for Translational Research, Osaka University Hospital, Osaka, Japan, [5]Department of Cardiac Physiology, National Cerebral and Cardiovascular Center Research Institute, Suita, Osaka, Japan, [6]SPring-8/JASRI, Sayo, Hyogo, Japan

Address for Correspondence; Professor Yoshiki Sawa

Department of Cardiovascular Surgery, Osaka University Graduate School of Medicine

2-2 Yamadaoka, Suita, 565-0871 Japan

Telephone; +81668793154, Facsimile; +81668793163

E-mail; sawa-p@surg1.med.osaka-u.ac.jp

Total word count: 5,328 words

CT-1353 Cell Transplantation Early Epub; provisional acceptance 12/04/2014

ABSTRACT

Functional and Electrical Integration of Induced Pluripotent Stem Cell-Derived Cardiomyocytes in a Myocardial Infarction Rat Heart

Higuchi T, Miyagawa S, Pearson JT, Fukushima S, Saito A, Tsuchimochi H, Sonobe T, Fujii Y,

In vitro expanded beating cardiac myocytes derived from induced pluripotent stem cells (iPSC-CMs) are a promising source of therapy for cardiac regeneration. Meanwhile, the cell-sheet method has been shown to potentially maximize survival, functionality and integration of the transplanted cells into the heart. It is thus hypothesized that transplanted iPSC-CMs in a cell-sheet manner may contribute to functional recovery *via* direct mechanical effects on the myocardial infarction (MI) heart.

: F344/NJcl-rnu/rnu rat were left coronary artery-ligated (n=30), followed by transplantation of Dsred-labeled iPSC-CMs cell-sheets of murine origin over the infarct heart surface. Effects of the treatment were assessed, including *in vivo* molecular/cellular evaluations using a synchrotron radiation scattering technique. Ejection fraction and activation recovery interval were significantly greater from day 3 onwards after iPSC-CMs transplantation compared to those after sham operation. A number of transplanted iPSC-CMs were present on the heart surface expressing cardiac myosin or connexin43 over two weeks, assessed by immunoconfocal microscopy, while mitochondria in the transplanted iPSC-CMs gradually showed mature structure as assessed by electronmicroscopy. Of note, X-ray diffraction identified 1,0 and 1,1 equatorial reflections attributable to myosin and actin-myosin lattice planes typical of organized cardiac muscle fibers within the transplanted cell-sheets at 4 weeks, suggesting cyclic systolic myosin mass transfer to actin filaments in the transplanted iPSC-CMs.

Transplantation of iPSC-CM cell-sheets into the heart yielded functional and electrical recovery with cyclic contraction of transplanted cells in the rat MI heart, indicating that this strategy may be a promising "cardiac muscle replacement" therapy.

Keywords: iPS cell; regeneration therapy; cell-sheet; synchrotron imaging

CT-1353 Cell Transplantation Early Epub; provisional acceptance 12/04/2014

INTRODUCTION

To increase the number of functional cardiomyocytes in the heart is a goal of regenerative therapy for advanced cardiac failure (14). It has been shown that induced pluripotent stem cells (iPSCs) differentiate into functional cardiomyocytes *in vitro* by specific culture regimens, suggesting that replacement of damaged cardiac tissue might be achieved by transplantation of iPSCs-derived cardiomyocytes (iPSC-CMs) into the damaged area using an appropriate cell-delivery method. Further, it has been shown that the cell-sheet method, in which a scaffold-free sheet-shaped cultured cell-cluster is placed on the surface of the heart, delivers a large number of the cells while preserving the functionality of the cells and the myocardium, indicating that the cell-sheet method may be an ideal delivery method of iPSC-CM to replace the damaged cardiac area (8,9,15). In fact, we reported that transplantation of iPSC-CMs into the heart by the cell-sheet method improves functional performance of the infarcted heart in pigs (5). However, in that study (5), synchronous contraction of the transplanted iPSC-CMs as "cardiac myocytes" that express the regular, cyclic actin-myosin cross-bridge motion, which is the aim of this treatment, was not demonstrated due to the limitations of current image analysis methods *in vivo*.

Shiba et al. reported that the fluorescent signal of calcium sensor, GCaMP3, which has been genetically encoded in the cells prior to transplantation into the heart, was useful for visualizing spontaneous contraction of the transplanted cells in the heart *in vivo* (16). However, the calcium sensor signal does not necessarily correlate with normal cyclic actin-myosin cross-bridge motion. On the other hand, third generation synchrotron radiation (SPring-8, Hyogo, Japan) has been utilized to quantify actin-myosin cross-bridge dynamics in cardiac fibres of localized regions *in vivo* (12,17). We herein hypothesized that transplanted iPSC-CMs in a cell-sheet manner may contribute to functional recovery *via* direct mechanical

effects on myocardial infarction (MI) heart. We therefore explored functional and electrical integration of the transplanted iPSC-CMs in the acute MI rat heart using the latest imaging modality utilising synchrotron radiation from a third generation facility.

METHODS

Studies were performed with the approval of the ethics committee of Osaka University Graduate School of Medicine and the Animal Experiment Review Committee of the Japan Synchrotron Radiation Research Institute. All animals used in this study received care in compliance with the Guide for the Care and Use of Laboratory Animals (National Institutes of Health Publication No 85-23, revised 1996).

Cell-culture and cell-sheet generation

Germline-competent mouse iPSC-line 256H18 was established by introducing only *Oct3/4*, *Sox2*, and *Klf4* (without *c-Myc*), constitutively expressing red-fluorescent protein (Dsred) (generously contributed by Professor S Yamanaka, Kyoto University, Japan) (11). Maintenance of the 256H18 iPSCs and induction of cardiomyogenic differentiation was performed following the protocol established in Professor Yamanaka's and our laboratories, respectively (7,23). Briefly, the iPSCs were maintained on feeder layers of mitomycin C-treated mouse embryonic fibroblasts (Chemicon, Billerica, MA). Embryoid bodies (EBs) were then generated under the presence of 6-bromoindirubin-3′-oxime (Calbiochem, Darmstadt, Germany) (23).

The EBs were plated on 12-well temperature-responsive culture dishes (CellSeed, Tokyo, Japan) at 37°C with the EB number adjusted to 20 per well, thereafter the EBs were differentiated in the serum free medium with insulin-transferin-selenium-X (Invitrogen,

Carlsbad, CA). Subsequently, the dishes were removed to refrigerator set at 20°C, while scaffold-free iPSC-CM cell-sheets detached spontaneously from the dish surfaces (23). Cardiac troponin T positivity in this preparation assessed by immunohistolabelling was consistently 70-80% (7,23).

Generation of acute myocardial infarction (MI) model and cell-sheet transplantation

Female F344/NJcl-rnu/rnu rats of 6 weeks of age (Crea, Tokyo, Japan) were anaesthetized by inhalation of isoflurane (1.5%) and endotracheally intubated for mechanical ventilation. The left coronary artery was then permanently occluded under thoracotomy (3). Two weeks after the ligation, the cell-sheet generated by iPSC-CMs or mitomycin C-treated mouse embryonic fibroblasts were simply placed on surface of the left ventricle (LV, n=6 each) (6). Bupivacaine (1% in saline, 250 μl) was subcutaneously injected near the incision line to minimize the postoperative pain and the rats were then recovered in a temperature-controlled individual cage.

Transthoracic echocardiography analysis

Transthoracic echocardiography was performed using a system equipped with a 12-MHz transducer and SONOS5500 (Agilent Technologies, Palo Alto, CA) under isoflurane inhalation (1%). Diastolic/systolic dimensions (Dd/Ds), and ejection fraction (EF) of the LV were measured (n=6 each) (3).

Telemetry study

A telemetry transmitter with two electrodes (Data Sciences International) was implanted prior to the treatment (day 14 post-MI) under inhalation of 1.5% isoflurane (n=4 each) (3). Electrocardiogram was then continuously monitored over 7 days. Ventricular premature

contractions (VPC) were detected and the frequency of the VPC was expressed as the number of VPC per day divided by the daily cumulative heart beats.

Electrical potential mapping analysis

Electrical potential mapping study was performed under the repeated left thoracotomies in the same animal at day 2, 3, 4, 7, and 14 (n=4 each group). There was no repeated procedures-related morbidity or mortality. A sixty-four electrical potential mapping system (Alpha MED Scientific, Osaka, Japan) was directly placed on surface of the LV *via* the thoracotomy under general anaesthesia and endotracheal intubation with mechanical ventilation as above. The electrical potential was recorded as the calculated activation recovery interval (ARI) in the same animals at the indicated time-points (n=4 each group).

Synchrotron small-angle scattering study

The fundamentals of synchrotron small-angle scattering techniques for the investigation of cross-bridge dynamics in the intact heart are presented in detail elsewhere (17). In brief, total thoracotomy was performed under general anaesthesia and endotracheal intubation with mechanical ventilation as above at the synchrotron radiation facility SPring-8 (n=4 in iPSC-CMs treated rats and in MI-only rats) as described in detail elsewhere (13). Cardiac catheterisation was performed to allow continuous LV pressure-volume recordings simultaneous with all SAXS and arterial pressure recordings. Pressure-volumetry was used to establish the timing of the cardiac cycle in all treatment periods and to permit assessment of actin-myosin contributions to global LV function. Heart rate (HR) was determined from the interval between end-diastolic (ED) events in the pressure-volume loops. Hemodynamic data were recorded using CHART (v5.5.6, ADInstruments, NSW) at a sampling rate of 1000/s.

A collimated quasi-monochromatic beam with 0.08 nm wavelength (15 keV),

dimensions 0.2 × 0.1mm (horizontal × vertical) and beam flux ~10^{12} photons/s (ring current 90–100 mA) was focused on the surface myocardium at an oblique tangent (rat ~3m from the detector). SAXS sequences (12 bit, 144 × 150 pixels) each lasting <2.1s were collected at a sampling interval of 15 ms with the aid of an image intensifier (V5445P, Hamamatsu Photonics, Hamamatsu, Japan) and a fast charge-coupled device camera (C4880-80-24A, Hamamatsu Photonics). Patterns were then digitally recorded using HiPic32 software (v5.1.0 Hamamatsu Photonics). With rats in a supine position, X-ray diffraction profiles were recorded vertically through the iPSC-CMs cell-sheet grafts and infarcted myocardium of the anterior LV wall of the exposed *in situ* beating hearts (12). Periodically between diffraction recordings a laser aligned with the X-ray beam was used to determine the point of path trajectory at which the beam also passed through normal myocardium. Diffraction patterns obtained from in situ iPSC sheets were of lower intensity compared to normal myocardium (remote regions) and easily distinguished on the basis of established cardiac fibre-intensity peak orientations (21).

Using custom software the average radial line profile around the centre of the spectrum was calculated using a three point background curve fitting process with manual definition of peak spectra limits. Background subtraction was then performed between user-defined inner and outer limits on either side of the 1,0 and 1,1 reflections. The integrated intensity of the 1,0 and 1,1 reflection intensities was then determined from the areas under the reflection peaks, defined as $I_{1,0}$ and $I_{1,1}$ respectively.

Enzyme-linked immunosorbent assay (ELISA)

Culture supernatants of cell-preparation were centrifuged to remove debris and cells. Content of vascular endothelial growth factor (VEGF) and hepatocyte growth factor (HGF) in the undiluted culture supernatants was determined with an ELISA kit (R&D Systems, MN, USA).

Immunohistolabelling analysis

Under anaesthesia by 5% isoflurane inhalation, heart was promptly excised, immersed in 4% paraformaldehyde, cut transversely and then frozen (n=5 each group). Ten μm-cryosections were labeled with monoclonal anti-cardiac myosin (Molecular Probes, Eugene, OR, USA), or monoclonal anti-connexin(Cx)43 (Millipore, Billerica, MA, USA) antibodies. The labelled sections were again labelled by the secondary antibodies (AlexaFluor488, or AlexaFluor594 phalloidin, Invitrogen), counterstained with 6-diamidino-2-phenylindole (DAPI, Invitrogen) and then assessed by immunoconfocal microscopy (FV1000D, Olympus, Tokyo, Japan)

Electron microscopy analysis

Sliced cardiac tissues were fixed with 2% glutaraldehyde in 0.1 mM phosphate buffer (pH 7.4) for 60 minutes at 4°C, washed and immersed overnight in PBS at 4°C, and fixed in 1% buffered osmium tetroxide, then dehydrated through graded ethanol and embedded in epoxy resin. Ultrathin sections (85 nm) were double-stained with uranyl acetate and lead citrate, and were observed under electron microscopy (H-7600; Hitachi, Tokyo, Japan).

Statistical analysis

All values were expressed as mean±standard deviations. Contents of VEGF and HGF in the supernatant of the four different cultures were compared by one-way ANOVA followed by Bonferroni's test for individual significant difference. Frequency of the VPC, ARI and LVEF were compared by two-way ANOVA followed by Bonferroni's tests for individual significant differences. $P < 0.05$ was considered to be statistically significant.

RESULTS

iPSCs-derived cardiomyocytes as a source of potential paracrine effects

It has been shown that cell transplantation into the heart produces "paracrine effects", in which the transplanted cells release a variety of protective factors into the adjacent native cardiac tissue to enhance native regenerative process, such as neo-angiogenic, anti-fibrotic, or anti-apoptotic effects (2). Capacity to release protective factors, such as VEGF and HGF, which have been shown to be the most important factors in the paracrine effects, were investigated here *in vitro*. Supernatant of the culture dishes of iPSC-CMs and fibroblasts was collected to measure concentration of VEGF and HGF by ELISA, showing that concentration of VEGF and HGF was not significantly different in the conditioned medium of the iPSC-CMs and the fibroblasts, suggesting potential "paracrine effects" of the iPSC-CM transplantation therapy.

Electrical integrity and functional recovery after cell-sheet transplantation in vivo

Cell-sheet method has been shown to transplant abundant somatic-tissue derived cells into the heart, which can be integrated into the cardiac tissue with minimal damage to the transplanted cells and to the myocardium (9). Functional integration of cell-sheets generated by iPSC-CM into the heart is, however, poorly understood. We speculate that similarity of the phenotype and/or character of the iPSC-CM to the native CM might result in a better integration into the native cardiac tissue compared to somatic tissue-derived cells.

Scaffold-free cell-sheets generated by Dsred-labeled iPSC-CMs of mouse origin were transplanted into the nude rat heart that had been subjected to permanent occlusion of the left coronary artery prior to the cell-sheet transplantation. The cell-sheet generated by Dsred-labelled fibroblasts, were used as controls. Electrical integrity and arrhythmogenicity were assessed by daily Holter ECG monitoring and 64-channel electrical potential mapping. In addition, global cardiac function was serially assessed by transthoracic echocardiography.

Electrical potential mapping identified multiple ectopic excitations over the cell-sheet transplanted area in the iPSC-CM group until day 2 (day 16 post-MI), which gradually disappeared from day 3 onwards (day 17 post-MI) (Figure 1A). In contrast, transplantation of the cell-sheet derived from fibroblasts, or MI-only rarely induced ectopic excitations over the study period. Ventricular premature contractions more frequently occurred post-iPSC-CM cell-sheet transplantation than those post-sham operation (Figure 1B). In addition, ARI was significantly less in the iPSC-CM group than the other groups from day 3 onwards (day 17 post-MI) (Figure 2A). Moreover, LVEF was significantly greater in the iPSC-CM group than the other groups between day 3 and day 14 (day 17 and day 28 post-MI) (Figure 2B). These findings indicate that the transplanted cell-sheets of iPSC-CMs generated functional and electrical integration into the acute MI rat heart more rapidly than those of fibroblasts.

In vivo recording of actin-myosin cross-bridge activity in the transplanted iPSC-CMs in the heart

While transplantation of iPSC-CM into the rat infarcted heart was shown to induce functional and electrical recovery, mechanical or functional behavior of each transplanted iPSC-CMs in the infarcted heart remains unclear. Actin-myosin cross-bridge interactions in the transplanted iPSC-CM in the rat infarcted heart was therefore investigated using fast synchrotron small-angle X-ray scattering.

At 4 weeks after the transplantation of iPSC-CM cell-sheets on the surface of the infarcted heart (6 weeks post-MI), the rats were subjected to removal of thoracic wall for the synchrotron study. X-ray diffraction profiles were recorded vertically through the iPSC-CM grafts and infarcted myocardium of the anterior LV wall of the *in situ* beating hearts. It was found that 1,0 and 1,1 equatorial reflections attributable to myosin and actin-myosin lattice